OXFORD GENETICS

GENETICS, 2023, 225(3), iyad164
https://doi.org/10.1093/genetics/iyad164
Advance Access Publication Date: 20 September 2023
Brief Investigation

Spenito-dependent metabolic sexual dimorphism intrinsic to fat storage cells

Arely V. Diaz,[1] Daniel Stephenson,[2] Travis Nemkov,[2] Angelo D'Alessandro,[2] Tânia Reis[1,*]

[1]Division of Endocrinology, Metabolism and Diabetes, Department of Medicine, University of Colorado Anschutz Medical Campus, Aurora, CO 80045, USA
[2]Department of Biochemistry and Molecular Genetics, University of Colorado Anschutz Medical Campus, Aurora, CO, 80045, USA

*Corresponding author: Division of Endocrinology, Metabolism and Diabetes, Department of Medicine, University of Colorado Anschutz Medical Campus, Aurora, CO 80045, USA. Email: tania.reis@cuanschutz.edu

Metabolism in males and females is distinct. Differences are usually linked to sexual reproduction, with circulating signals (e.g. hormones) playing major roles. In contrast, sex differences prior to sexual maturity and intrinsic to individual metabolic tissues are less understood. We analyzed *Drosophila melanogaster* larvae and find that males store more fat than females, the opposite of the sexual dimorphism in adults. We show that metabolic differences are intrinsic to the major fat storage tissue, including many differences in the expression of metabolic genes. Our previous work identified fat storage roles for Spenito (Nito), a conserved RNA-binding protein and regulator of sex determination. Nito knockdown specifically in the fat storage tissue abolished fat differences between males and females. We further show that Nito is required for sex-specific expression of the master regulator of sex determination, Sex-lethal (Sxl). "Feminization" of fat storage cells via tissue-specific overexpression of a Sxl target gene made larvae lean, reduced the fat differences between males and females, and induced female-like metabolic gene expression. Altogether, this study supports a model in which Nito autonomously controls sexual dimorphisms and differential expression of metabolic genes in fat cells in part through its regulation of the sex determination pathway.

Keywords: Nito; Sxl; Tra; *Drosophila melanogaster*; fruit fly; larva; fat body; metabolism; sexual dimorphism; sex differences; sex determination

Introduction

Males and females differ fundamentally with regard to metabolism (Mauvais-Jarvis 2015), but the underlying molecular mechanisms regulating these differences are incompletely understood. Most studies focus on the importance of sex chromosomes and sex hormones on regulating these differences, especially how signals from the gonads influence metabolism in other tissues (e.g. estrogen) (Bjune et al. 2022). Less is known about the effects of sex chromosome constitution in tissues not directly involved in sexual reproduction and to what extent these differences contribute to the sexual dimorphisms observed at the organismal level, including metabolic dimorphism (Link et al. 2013).

Metabolic dimorphism is well documented in sexually mature adult *Drosophila melanogaster* (reviewed in Shingleton and Vea (2023). Differences in triglyceride storage and breakdown (Schwasinger-Schmidt et al. 2012; Sieber and Spradling 2015; Wat et al. 2020), lipid composition (Parisi et al. 2011), and obesogenic responses to diets (De Groef et al. 2022; Kubrak et al. 2022) have all been identified. Furthermore, dietary switches can affect males and females differently (Vargas et al. 2010; Reddiex et al. 2013; Gillette et al. 2020). Some behaviors that change metabolic outcomes are also dimorphic: feeding and locomotor activities differ between the sexes in certain dietary and physiological conditions across the lifespan (Shaw et al. 2000; Isaac et al. 2010; White et al. 2010; Brown et al. 2022). As in humans, most metabolic dimorphisms in flies have been linked to circulating signals between different tissues. Sex peptide is a hormone found in sperm that influences female physiology and behavior after mating, including feeding (Carvalho et al. 2006) and nutrient utilization (Koppik and Fricke 2022). Sex differences in adult *Drosophila* courtship behaviors are controlled in part by circulating male-specific proteins produced by the fat body (FB) (Dauwalder et al. 2002), a specialized tissue that performs energy storage functions equivalent to mammalian liver and white adipose tissue. Finally, sex differences in carbohydrate metabolism in cells of the adult intestine are controlled by signaling from the male gonad and couple diet with sperm production (Hudry et al. 2019).

For any species, less is known about intrinsic, tissue-specific sex differences during development (reviewed in Shingleton and Vea (2023)). For those differences that are manifested before animals are sexually mature, it is not clear if they impact lifespan, healthspan, and/or reproduction later in life. We previously identified and characterized how the SPEN family of RNA-binding proteins in *Drosophila*—Split ends (Spen) and Spenito (Nito)—act in the larval FB to maintain proper fat levels (Reis et al. 2010; Hazegh et al. 2017). A connection between sex determination and fat storage came from parallel findings that Nito is also required for proper sex determination via regulation of alternative splicing in the canonical *Sex-lethal* (*Sxl*) pathway (Yan and Perrimon 2015; Haussmann et al. 2016; Lence et al. 2016; Kan et al. 2017; Knuckles et al. 2018). As a first step to understanding

Received on 05 June 2023; accepted on 16 August 2023

intrinsic sex differences during *Drosophila* development, here, we measure metabolic differences in larvae—which are sexually immature—and explore roles for Nito and the Sxl pathway in these differences.

Materials and methods

Fly strains and husbandry

w^{1118} [Bloomington *Drosophila* Stock Center stock number (BL) 3605], w^{1118}; *cg > GAL4* (*BL 7011*), *y1 sc* v1 sev21*; *P{TRiP.HMS02013}attP40* (BL 56851, UAS-Nito-RNAi), *y1 sc* v1 sev21*; *P{TRiP.HMS00166}attP2* (*BL 34848*, UAS-Nito-RNAi), *y1 sc* v1 sev21*; *P{TRiP.HMS05713}attP40* (BL 67852, RFP-RNAi), w^{1118}; *P{UAS-GFP.nls}14* (BL 4775) and w^{1118}; and *P{UAS-tra.F}20J7* (BL 4590) were obtained from the Bloomington *Drosophila* Stock Center. All lines were backcrossed to the w^{1118} stock. Unless otherwise specified, all animals were reared at 25°C and 60% humidity and fed a modified Bloomington media [1 L: yeast 15.9 g, soy flour 9.2 g, yellow cornmeal 67.1 g, light malt extract 42.4 g, agar 5.3 g, light corn syrup 90 g, propionic acid 4.4 mL, Tegosept (Apex Bioresearch Products #20–258, 380 g in 1 L 100% ethanol) 8.4 mL]. Experimental media (1 L: yeast 35 g, soy flour 9.2 g, yellow cornmeal 65 g, light malt extract 42.4 g, agar 5.3 g, light corn syrup 70 mL, propionic acid 4.4 mL, Tegosept 8.4 mL) was made fresh each week and used for no longer than 1 week. Crosses were made with 100–120 virgin females with 50–60 males. Eggs were collected for 5 h on grape plates at 25°C and 60% humidity and 50 first-instar larvae were transferred 22–24 h later into a vial with experimental media.

Density assay

For sexed density assays, 50 wandering third-instar larvae of each sex were sorted per sample prior to the assay. Density assays were then performed as previously described (Reis et al. 2010; Hazegh and Reis 2016). For each experiment, genetic background controls were also tested by crossing either the siblings of each UAS-line or the driver line with w^{1118}. The resulting male and female progeny showed similar dimorphism to controls, and there were no significant effects of the insertions on density. All experimental conditions and genotypes were analyzed with 8–9 independent samples. Two-way ANOVA with Šídák's (Fig. 1 or Tukey's tests (Figs. 2 and 3) was used to calculate statistical significance with GraphPad Prism software.

Feeding assay

Twenty sexed, early third-instar larvae were used per sample to measure intake of yeast containing 0.5% food dye (FD&C Red #40) on an agar plate at 25°C for 30 min, as previously described (Reis et al. 2010). Four independent biological samples were analyzed by paired *t*-test using GraphPad Prism software.

Activity assay

Fifteen sexed, prewandering third-instar larvae were collected and tracked for movement as previously described (Mosher et al. 2015). Four independent samples were analyzed by Mann–Whitney and Kolmogorov–Smirnov tests using GraphPad Prism software.

Lipidomics

Sample preparation. Lipids were extracted via a protein crash modified from a previously described method (Mosher et al. 2015; Reisz et al. 2019. Wildtype whole larvae [$n = 10$, biological experiment repeated five times per each condition (male vs female)] were homogenized and extracted at 15 mg/mL ratio in ice-cold methanol. Following homogenization, samples were vortexed for 30 min, followed by centrifugation at 12,700 revolutions per minute (RPM for 10 min at 4°C. One hundred µL of supernatant was transferred to a new autosampler tube for sample analysis.

UHPLC-MS data acquisition and processing. Analyses were performed as previously published (Pang et al. 2022). Briefly, the analytical platform employs a Vanquish UHPLC system (Thermo Fisher Scientific, San Jose, CA, USA) coupled online to a Q Exactive mass spectrometer (Thermo Fisher Scientific, San Jose, CA, USA). Lipid extracts were resolved over an ACQUITY HSS T3 column (2.1 × 150 mm, 1.8 µm particle size) (Waters, MA, USA) using an aqueous phase (A) of 25% acetonitrile and 5 mM ammonium acetate and a mobile phase (B) of 90% isopropanol, 10% acetonitrile, and 5 mM ammonium acetate. For negative mode analysis, the chromatographic gradient was as follows: 0.3 mL/min flowrate and 30% B at 0 min, 0.3 mL/min flowrate and 100% B at 3 min, 0.3 mL/min flowrate and 100% B at 4.2 min, 0.4 mL/min flowrate and 30% B at 4.3 min, 0.4 mL/min flowrate and 30% B at 4.5 min, and 0.3 mL/min flowrate and 30% B at 5 min. For positive mode analysis, the chromatographic gradient was as follows: 0.3 mL/min flowrate and 10% B at 0 min, 0.3 mL/min flowrate and 95% B at 3 min, 0.3 mL/min flowrate and 95% B at 4.2 min, 0.45 mL/min flowrate and 10% B at 4.3 min, 0.4 mL/min flowrate and 10% B at 4.5 min, and 0.3 mL/min flowrate and 10% B at 5 min. The Q Exactive mass spectrometer (Thermo Fisher) was operated in positive ion mode, scanning in full MS mode (2 µscans) from 150 to 1500 m/z at 70,000 resolution, with 4 kV spray voltage, 45 sheath gas, and 15 auxiliary gas. When required, dd-MS2 was performed at 17,500 resolution, AGC target = $1e^5$, maximum IT = 50 ms, and stepped NCE of 25, 35 for positive mode, and 20, 24, and 28 for negative mode. Calibration was performed prior to analysis using the Pierce Positive and Negative Ion Calibration Solutions (Thermo Fisher Scientific).

Data analysis

Acquired data were converted from raw to mzXML file format using Mass Matrix (Cleveland, OH, USA). Samples were analyzed in randomized order with a technical mixture injected interspersed throughout the run to qualify instrument performance. Lipidomic data were analyzed using LipidSearch 4.0 (Thermo Scientific), which provides lipid identification on the basis of accurate intact mass, isotopic pattern, and fragmentation pattern to determine lipid class and acyl chain composition. Peak areas were extracted in tabular format and processed in Excel. To calculate total lipid class composition, lipids were categorized by determined lipid class and summed together. The same approach was used for acylchain length and total degrees of unsaturation. We note that while our lipidomic data are direct and quantitative in a relative sense (comparing amounts collected from animals in the same experiment in the same batch), they are not absolutely quantitative, since we do not include isotopically labeled standards. Graphs, heat maps, and statistical analyses (paired *t*-test) and partial least squares-discriminant analysis (PLS-DA) were performed using MetaboAnalyst 5.0 (Pang et al. 2022).

RNA sequencing

Sample preparation. Total RNA was extracted from 50 third-instar FBs dissected from sexed larvae using 500 µL of TRIzol (Ambion Cat #15596018) and purified using the Direct-zol Miniprep Plus kit digested with DNase I (Zymo Cat #R2072). RNA sequencing and library prep was performed at the University of Colorado Anschutz medical campus Genomics Core. Libraries were

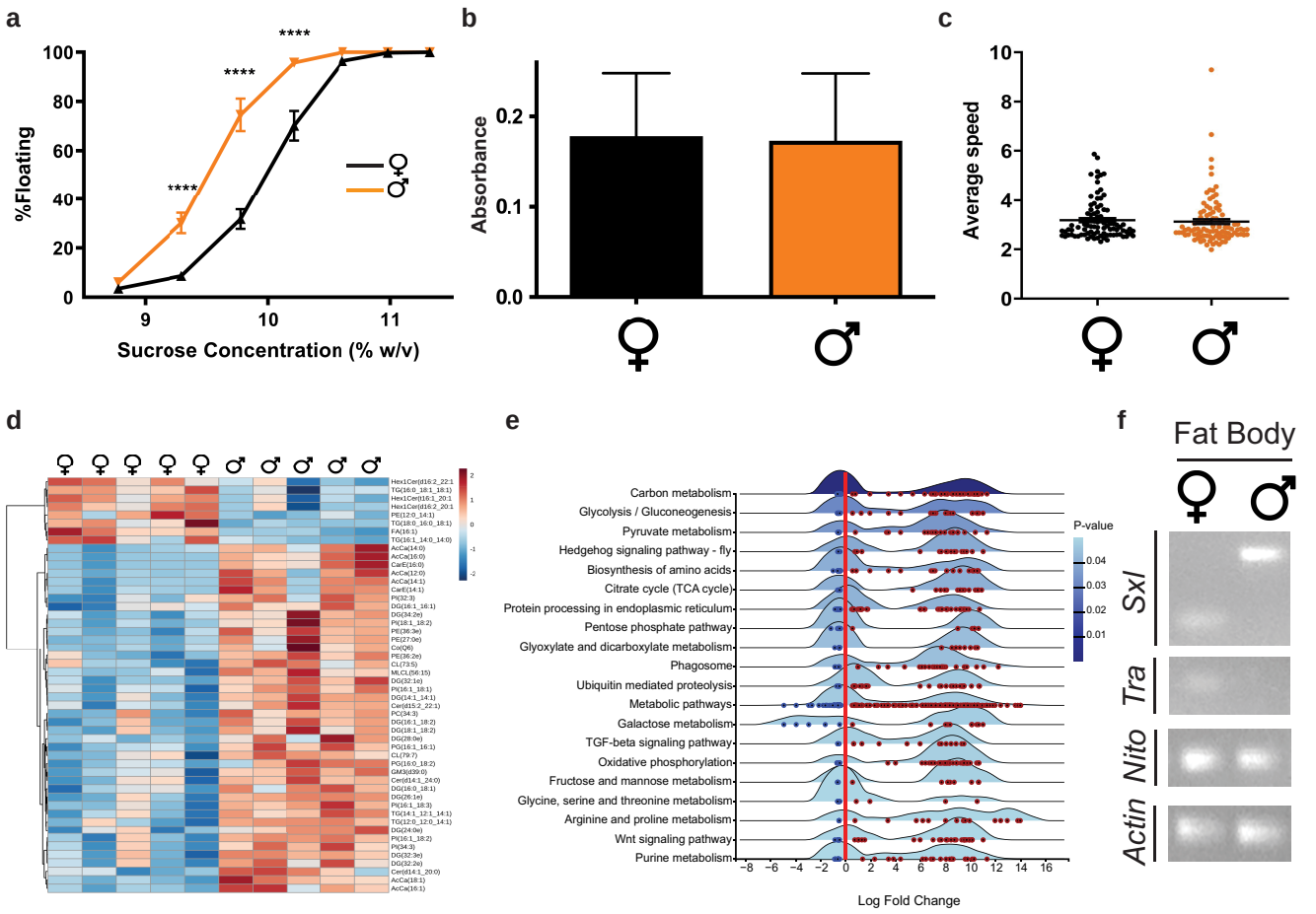

Fig. 1. Sexual dimorphism in metabolism and metabolic gene expression. a) Percent floating male or female larvae in increasing sucrose densities (percent weight/volume). $n = 9$ biological replicates per sample, 50 larvae per replicate. P values represent results from two-way ANOVA (****$P < 0.0001$). Error bars represent SEM. b) Absorbance at 520 nm as a measure of food intake. $n = 4$ biological replicates per sample, 20 larvae per replicate. Error bars represent SD. c) Average larval speed, pixels/s. $n = 4$ biological replicates per sample, 15 larvae per replicate. Error bars represent SEM. d) The heat map shows the top 50 most significant ($P < 0.05$, unpaired t-test) lipidomic differences between male and female larvae. Z-score-normalized lipid values are indicated from dark blue to dark red according to lowest or highest abundance, respectively. $n = 5$ biological replicates per sample, 10 larvae per replicate. Due to normalization, separate rows cannot be compared with one another. e) Ridgeline Enrichment Diagram for KEGG functions from the RNA-seq gene list with significant differential gene expression (adjusted $P < 0.05$). f) RT-PCR products representing the indicated transcripts in RNA extracted from male or female larval fat bodies were separated on 2% agarose gels. *Actin* is a loading control. $n = 3$ biological replicates; shown is a representative experiment.

prepped according to the manufacturer's protocol using the Universal Plus mRNA-Seq library preparation kit with NuQant (TECAN Cat #0520-24).

Data acquisition and processing: libraries were sequenced with an Illumina NovaSeq 6000 system. Transcriptome analysis was performed using pseudo-alignment with Salmon (Patro et al. 2017) using the *D. melanogaster* transcriptome (version dmel_r6.48_FB2022_05). DESeq2 (Love et al. 2014) (version 1.40.1) was used for differential expression analysis. Kyoto Encyclopedia of Genes and Genomes (KEGG pathway analysis of the entire list of significantly changed genes was performed using ExpressAnalyst (Liu et al. 2023). Pathway enrichment of the top 25 up- and downregulated genes was performed using FlyMine (version 53) (Lyne et al. 2007), which uses KEGG and Reactome pathways.

RT-PCR

Total RNA was extracted from 50 third-instar FBs dissected from sexed larvae using 500 µL of TRIzol (Ambion Cat #15596018) and purified using the Direct-zol Miniprep Plus kit digested with DNase I (Zymo Research Cat #R2072). Total purified RNA was used for reverse transcription using SuperScript IV Reverse transcriptase (Invitrogen Cat #18090010). Semiquantitative PCR was performed using *Taq* DNA polymerase with standard *Taq* buffer (New England BioLabs Cat #M0273S). PCR products were analyzed on 2% Agarose gels with 0.5 ng/L ethidium bromide using a 1 kb Plus DNA Ladder (New England BioLabs Cat #N3200S) for size reference. Primer sequences: Nito, 5′ CGCAGTTAACTTTCGACGCA 3′ and 5′ AGTTCCGGGGATTCACTTCC 3′; Sxl, 5′ GTGGTTATCCCCC ATATGGC 3′ and 5′ GATGGCAGAGAATGGGAC 3′; Tra, 5′ GGAAC CCAGCATCGAGATTC 3′ and 5′ ATCGCCCATGGTATTCTCTTTC 3′; Actin, 5′ TTGATGTCACGGACGATTTC 3′ and 5′ TTGATGTCA CGGACGATTTC 3′; Yp3 primer pair 1, 5′ AATGACCGACTGAAG CCGAC 3′ and 5′ TGGACTTGATAATCCAGACGGG 3′; and Yp2 primer pair 1, 5′ GCACCCTTTGCGTTATGGC 3′ and 5′ TAGAGCTTG TCCAACAGCGTA 3′.

RT-qPCR

Total RNA was extracted from dissected FB from 50 male or female larvae using 500 µL of TRIzol (Ambion Cat #15596018) and

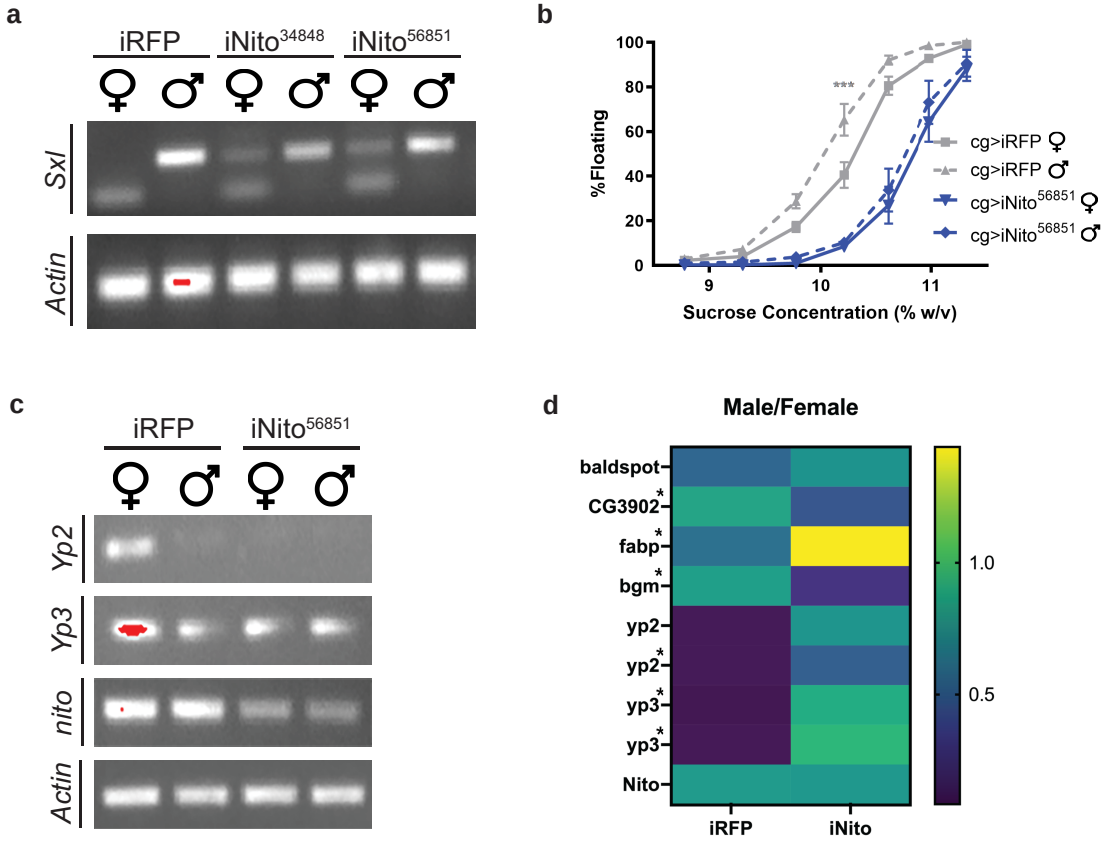

Fig. 2. Nito is required for metabolic sexual dimorphism in the FB. a and c) RT-PCR products representing the indicated transcripts in RNA extracted from Nito or control (RFP) KD male or female larval fat bodies were separated on 2% agarose gels. *Actin* is a loading control. $n = 3$ biological replicates; shown is a representative experiment. b) Percent floating larvae in increasing sucrose densities (percent weight/volume). FB-specific Nito KD (cg > iNito, blue) compared with KD control (cg > iRFP, gray). Females are shown in solid lines and males in dashed lines. $n = 8$ biological replicates per sample, 50 larvae per sample. *P* values represent results from two-way ANOVA, ***$P < 0.001$. Error bars represent SEM. d) Heatmap of male-vs-female differences in transcript levels of select metabolic genes upon FB-specific Nito KD or control KD (RFP) as measured by RT-qPCR. * indicates statistical significance according to multiple paired *t*-test.

purified using the Direct-zol Miniprep Plus kit digested with DNase I (Zymo Research Cat #R2072) treatment. One and a half µg of total purified RNA was used for reverse transcription using SuperScript IV Reverse transcriptase (Invitrogen Cat #18090010). qPCR was performed using PowerUp SYBR Green Master Mix (Applied Biosystems Cat #A25742). Reactions were run in an Applied Biosystems Step One Plus qPCR machine using the ΔΔCT method, using *actin5c*, *alpha-tubulin84B*, *cg5321*, and *cg12703* as endogenous controls. Three RT-qPCRs from three independent biological replicates were performed. *P* values were obtained by multiple paired *t*-test using Prism 6 software. Primer sequences are listed above (for *yp3*, *yp2*, *nito*, and *actin5c*,) or as follows: Yp2 primer pair 2, 5′ ATCAGGGGCTACATTGTCGG 3′ and 5′ CCTGGATGAAGATGGTGACCT 3′; Yp3 primer pair 2, 5′ CCTACGTCCAGAAGTACAACCT 3′ and 5′ TTGGCGGATTTCCA TTGGTCA 3′; fabp, 5′ CACAGTGGAGGTGACCTTGG 3′ and 5′ GATGCTCTTGACGTTGCGAC 3′; bgm, 5′ TGGACAAGATTCACG CCATTC 3′ and 5′ CGACCACCTGTAGTAGCCATC 3′; CG3902, 5′ CTCACCGACGATGAGAAAATGA 3′ and 5′ CACGGAGGGATCGA ATTTGTG 3′; baldspot, 5′ GTGGTCAGCACTTTATGCAAAAT 3′ and 5′ GTGGAAGAGTCCGTAGTGACG 3′; alpha-tubulin48B, 5′ AACCTGAACCGTCTGATTGG 3′ and 5′ GGTCACCAGAGGGAAG TGAA 3′; CG5321, 5′ TAACTTCGATACCCGCATCC 3′ and 5′ CGAAA CATCGCTCCTTTAGC 3′; and CG12703, 5′ CGAAACATCGCTC CTTTAGC 3′ and 5′ TGGTGGAGAGCACCATCATA 3′.

Results and discussion

Metabolic sexual dimorphism in Drosophila larvae

The larval developmental stage precedes pupae and adults. We first compared larval body fat using a density-based assay (Reis et al. 2010). Animals of the commonly used w^{1118} experimental genetic background were sorted by sex and analyzed separately. Significant sexual dimorphism was observed, with males having lower overall density than females (Fig. 1a), indicative of higher overall fat levels. Intriguingly, this sex difference is opposite to that found in adults (Rideout et al. 2015; Sieber and Spradling 2015; Bednářová et al. 2018). The adult dimorphism develops gradually over time: fat levels are equivalent in newly enclosed males and females (Wat et al. 2020). Female adults consume more food than males, with mated females eating even more (Carvalho et al. 2006; Barnes et al. 2008; Kubrak et al. 2022). We found no significant sex difference in larval food consumption or locomotor activity (Fig. 1b and c), suggesting that these behaviors do not contribute to the observed differences in fat levels.

To ask if fat dimorphism at the organismal level reflects dimorphism at the molecular level, we performed lipidomic analysis on whole male or female larvae. Indeed, PLS-DA revealed clustering in lipidomic profiles of male and female larvae (Supplementary Fig. 1). Males had higher levels of acylcarnitines, diacylglycerols,

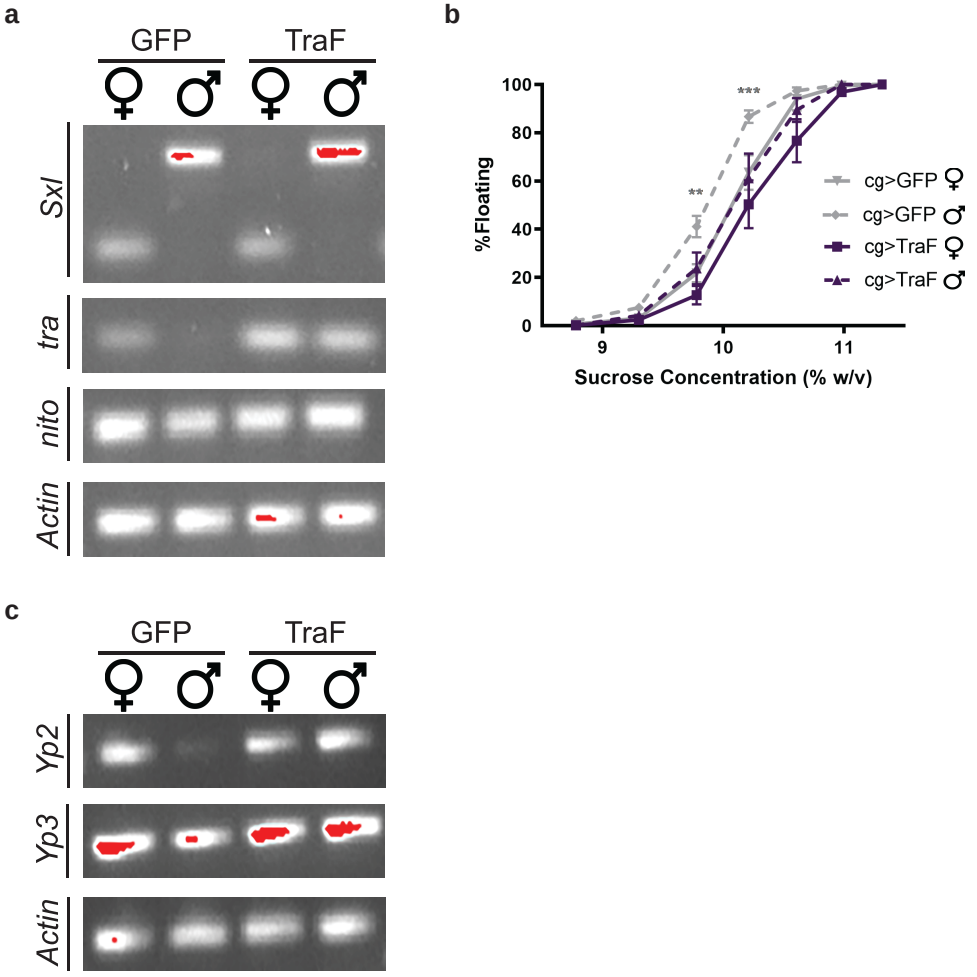

Fig. 3. FB-specific TraF expression feminizes metabolism in male larvae. a and c) RT-PCR products representing the indicated transcripts in RNA extracted from TraF- and GFP-overexpressing male and female larval fat bodies. *Actin* is a loading control. $n = 3$ biological replicates; shown is a representative experiment. b) Percent floating larvae in increasing sucrose densities (percent weight/volume). FB-specific TraF overexpression (cg > TraF, purple) compared with overexpression control (cg > GFP, gray). Females are shown in solid lines and males in dashed lines. $n = 9$ biological replicates per sample, 50 larvae per sample. *P* values represent results from two-way ANOVA, $^{**}P < 0.01$, $^{***}P < 0.001$. Error bars represent SEM.

and several triacylglycerols (Fig. 1d; Supplementary Fig. 1 and Table 1), consistent with our indirect body fat results from the density assay. The male-specific increase in acylcarnitines observed in the lipidomics suggests increased mobilization for fatty acid oxidation: males also had higher levels of acyl-CoA pools, indicating either increased use of, or a blockage within, β-oxidation. In the absence of kinetic analysis, e.g. isotope fluxes, these data indicate the latter might be true, especially in light of the higher degree of unsaturation within acyl chains across the entire lipidome observed in males (Supplementary Table 1), which would require additional enzymatic steps for the process to proceed. This scenario would result in a blockage and accumulation of acyl-CoA and acylcarnitines in males.

Under the premise that metabolic differences at the organismal level reflect gene expression changes in the FB, we isolated RNA from FBs from male and female larvae and performed RNA sequencing (RNA-seq). KEGG pathway enrichment analysis identified numerous metabolic pathways that were significantly enriched (Fig. 1e). The three most significantly enriched pathways were carbon metabolism, glycolysis/gluconeogenesis, and pyruvate metabolism (Fig. 1e). Looking specifically at the 25 genes that were most significantly increased and the 25 that were most significantly decreased, in males vs females, we saw significant enrichment for specific pathways involving lipid metabolism (Supplementary Fig. 2 and Table 2). Notable examples of downregulated genes include *Phospholipase A2 group III* (*GIIIspla2*), *Glycerophosphate oxidase 1* (*Gpo1*), the fatty acid elongase *Baldspot* (Senyilmaz et al. 2015), the long-chain-fatty-acid-CoA ligase *heimdall* (*hll*) (Thimgan et al. 2015), the short-chain 2-methylacyl-CoA dehydrogenase *CG3902*, the known or predicted fatty acid binding proteins *fabp* and *CG4586*, and the lipase family genes *magro* (*mag*) (Sieber and Thummel 2012), *doppelganger von brummer* (*dob*) (Gronke et al. 2005), *Yolk protein 2* (*Yp2*), and *Yolk protein 3* (*Yp3*) (Horne et al. 2009) (Supplementary Table 2). We previously identified *fabp* mutants as accumulating extra stored fat in an unbiased screen of mutant larvae (Reis et al. 2010), and *mag* mutant adults accumulate stored lipids (Sieber and Thummel 2012). These differences in gene expression are thus consistent with the observed increase in body fat in males and with our lipidomic results. Notably, we saw little overlap with published adult sex-specific differences in metabolic genes (Wat et al. 2020) (Supplementary Table 2), consistent with the phenotypic contrast in adults, where females are fatter.

Yp3 was the most significantly downregulated transcript in male FBs (Supplementary Table 2). In the vitellogenesis process, yolk proteins synthesized in the FBs of adult females are secreted

into circulation and ultimately taken up by developing oocytes to become the major protein components of yolk (reviewed in Bownes (1994)). Following fertilization, the energy stored in yolk fuels embryogenesis. Yolk proteins lack conserved residues required for lipase activity (Horne et al. 2009) but are major components of the lipid droplet proteome (Cermelli et al. 2006) and have been proposed to transport lipids to oocytes (Bownes 1992). Yp3 is among the most abundant larval proteins (Casas-Vila et al. 2017) and was the most strongly downregulated larval hemolymph protein upon starvation (Handke et al. 2013), further pointing to a role in larval organismal energy balance prior to oogenesis.

In our RNA-seq data, we noticed sex-specific FB expression of Sxl and a downstream sex determination gene, *transformer* (*tra*) (Supplementary Table 2). RT-PCR confirmed the presence of the female-specific Sxl isoform exclusively in the female FB and the male-specific isoform exclusively in the male FB (Fig. 1f). We interpret these results as evidence that the canonical sex determination pathway operates in larval FB cells. Gonads in the larva are embedded in the FB (Kerkis 1931; Sonnenblick 1941) and are much bigger (more than three times) in males than in females (Kerkis 1931; Sonnenblick 1941). Thus, we speculate that, analogous to the extra stores adult females require to support ovarian development (Aguila et al. 2013), male larvae might need more stored energy for gonad growth and development. Indeed, cytokinesis during spermatogenesis requires very-long-chain fatty acids or their derivative lipids (Szafer-Glusman et al. 2008), pointing to possible sex-specific lipid requirements during gametogenesis.

Nito regulates metabolic sexual dimorphism and sex determination in the FB

Due to Nito's role in sex determination, and because we observed sex-specific expression of sex-determinant genes in FB cells, we tested whether FB-specific depletion of Nito via RNAi alters the dimorphic expression of the sex determination gene Sxl. As expected, RNAi control animals expressed the respective male and female transcripts in the FB (Fig. 2a). However, upon Nito depletion, we observed the male Sxl isoform in female FBs (Fig. 2a). These expression patterns are consistent with equivalent effects of Nito depletion in the wing (Yan and Perrimon 2015) and with a masculinization of the female FB in the absence of Nito and support the hypothesis that Nito is required in FB cells to establish and/or maintain a sex-specific larval FB identity. Detection of both Sxl isoforms in female FBs only upon FB-specific Nito depletion also excludes the possibility that the dimorphic expression we observed in w^{1118} larvae solely reflects gonad-derived transcripts.

Using mixed-sex measurements, we previously found that FB depletion of Nito alters larval body fat (Hazegh et al. 2017). We repeated this analysis but separated larvae by sex. Larvae with Nito-depleted FBs were lean, but there was no longer a significant difference between males and females (Fig. 2b). At the molecular level, depleting Nito also eliminated the sex differences we had identified by RNA-seq in levels of transcripts encoding metabolic enzymes. Specifically, in confirmation of our RNA-seq data, RT-PCR revealed increased levels of Yp2 and Yp3 in control females compared with males (Fig. 2c). In contrast, levels of Yp2 and Yp3 transcripts were similar in the Nito-depleted FB of males and females (Fig. 2c). RT-qPCR confirmed that Nito depletion significantly altered the gene expression dimorphism for Yp2, Yp3, *fabp*, CG3902, and the very-long-chain acyl-CoA synthetase *bubblegum* (*bgm*) (Sivachenko et al. 2016) (Fig. 2d). *bgm* mutants were also identified in our unbiased screen for fat larvae (Reis et al. 2010). These results are consistent with a role for Nito in promoting metabolic sexual dimorphism in the FB via differential expression of genes controlling metabolism.

Sex determination pathway effects on larval body fat

Our results indicate that metabolic sexual dimorphism is intrinsic to the FB. In other tissues, Tra controls the splicing of downstream targets that direct somatic female development and behavior, such as genitalia and courtship (Baker and Ridge 1980; Burtis and Baker 1989; Hoshijima et al. 1991). To ask directly if dimorphic gene expression in fat cells is sufficient to dictate sex-specific fat storage, we overexpressed the female determinant isoform of Tra (TraF) in male and female FBs. Consistent with Tra acting downstream of Sxl, there was no change in Sxl splicing or *nito* transcript levels (Fig. 3a). Strikingly, expression of TraF in FB of males and females resulted in leaner males and females than the GFP overexpression control (Fig. 3b). Consistent with metabolic feminization of males, following TraF overexpression, we observed increased levels of Yp2 and Yp3, similar to females (Fig. 3c). Sex-specific Yp2 and Yp3 expression in adults is known to require *tra* function (Belote et al. 1985). Our data show that this is also true in larval FBs. Tra was known to act in the FB to control dimorphism of larval body size via non–cell-autonomous insulin-like peptide signaling (Rideout et al. 2015). In adults, Tra promotes fat storage in females via control of hormone release from neurons (Wat et al. 2021). We interpret our data as evidence of Tra-dependent dimorphism in metabolic gene expression intrinsic to the larval FB.

Nito depletion and TraF overexpression both resulted in lean phenotypes and collapse of dimorphism. However, and as expected, FB-specific Nito depletion masculinized Yp2 and Yp3 expression in females and TraF overexpression feminized Yp2 and Yp3 expression in males (Figs. 2c and 3c). The lean phenotype observed upon Nito depletion is stronger than that following TraF expression (Figs. 2b and 3b). We previously characterized Nito's antagonistic role to Spen function in regulating fat levels and showed that Spen is not required in the FB for metabolic dimorphism (Hazegh et al. 2017). We therefore propose that Nito is required in two parallel pathways: one that regulates metabolism in a sex-specific manner and—together with its sibling, Spen—another that regulates metabolism in a sex-independent manner. For example, Nito knockdown (KD) has the same effect on expression of *baldspot* in both males and females (Supplementary Fig. 3), indicating that *baldspot* is regulated by Nito in a sex-independent manner.

Given Nito's role in alternative splicing via RNA modification with N^6-methyladenosine (m^6A) as part of the canonical sex determination pathway(Yan and Perrimon 2015; Haussmann et al. 2016; Lence et al. 2016; Kan et al. 2017), we predict that Nito-dependent m^6A modification of transcripts encoding key metabolic enzymes results in dimorphic expression and ultimately metabolic differences. Indeed, m^6A RNA modification in mice is an essential regulator of sex-specific differences in lipid metabolism (Salisbury et al. 2021). High levels of m^6A modification are present on lipogenic mRNAs in mice liver, with males having higher levels than females (Salisbury et al. 2021). Additionally, loss of m^6A in males leads to "feminization" of lipid composition (Salisbury et al. 2021). It is not known which m^6A targets control fat storage and how different components of the m^6A machinery contribute to this regulation.

Taken together, our data raise new questions, demanding a deeper understanding of how overall organismal dimorphic

differences result from a balance between intrinsic genetic vs hormonal differences and to what extent these differences influence healthspan and reproduction. Understanding these questions becomes even more important in the context of exogenous introduction of sex hormones and/or hormone blockers, such as hormonal therapies used as cancer treatments or as gender-affirming healthcare services.

Data availability

All fly lines used in this study are available upon request or can also be obtained through the Bloomington *Drosophila* Stock Center (Bloomington stock numbers and full genotypes are provided in the Materials and methods section). Raw gene expression data are available at Gene Expression Omnibus (GEO with the accession number GSE229991. All code relating to this project is available at https://github.com/rnabioco/reis-rbi-pilot-fat-body.

Supplementary material available at *GENETICS* online.

Acknowledgments

We would like to thank the Bloomington Stock Center (supported by the Office of the Director of the National Institutes of Health P40OD018537) for generously maintaining and providing fly stocks, FlyBase: A Drosophila Genomic and Genetic Database, version FB2022_05 (et al. 2022), and all the very generous members of our Fly Community. We would also like to thank Michael McMurray for his helpful comments and editing of the manuscript. We thank the CU AMC Sequencing Facility for preparing and sequencing the RNA samples, Jay Hesselberth for support with RNA-seq analysis, and Laura George, who performed preliminary studies on the dimorphism of Oregon R larvae.

Funding

A.V.D. was supported by the National Institute for General Medical Sciences of the National Institutes of Health (T32-GM136444 and F31GM149062), the Victor W. and Earleen D. Bolie Graduate Scholarship, and a CU Anschutz RNA Bioscience Initiative Scholar award. T.R. was supported by the National Institute of Diabetes and Digestive and Kidney Diseases of the National Institutes of Health (R01DK106177) and a Pilot Award from the RNA Biosciences Initiative of the University of Colorado Anschutz Medical Campus.

Conflicts of interest statement

The authors declare no conflict of interest.

Literature cited

Aguila JR, Hoshizaki DK, Gibbs AG. 2013. Contribution of larval nutrition to adult reproduction in *Drosophila melanogaster*. J Exp Biol. 216(Pt 3):399–406. doi:10.1242/jeb.078311.

Baker BS, Ridge KA. 1980. Sex and the single cell. I. On the action of major loci affecting sex determination in *Drosophila melanogaster*. Genetics 94(2):383–423. doi:10.1093/genetics/94.2.383.

Barnes AI, Wigby S, Boone JM, Partridge L, Chapman T. 2008. Feeding, fecundity and lifespan in female *Drosophila melanogaster*. Proc Biol Sci. 275(1643):1675–1683. doi:10.1098/rspb.2008.0139.

Bednářová A, Tomčala A, Mochanová M, Kodrík D, Krishnan N. 2018. Disruption of adipokinetic hormone mediated energy homeostasis has subtle effects on physiology, behavior and lipid status during aging in Drosophila. Front Physiol. 9:949. doi:10.3389/fphys.2018.00949.

Belote JM, Handler AM, Wolfner MF, Livak KJ, Baker BS. 1985. Sex-specific regulation of yolk protein gene expression in Drosophila. Cell 40(2):339–348. doi:10.1016/0092-8674(85)90148-5.

Bjune JI, Strømland PP, Jersin RA, Mellgren G, Dankel SN. 2022. Metabolic and epigenetic regulation by estrogen in adipocytes. Front Endocrinol (Lausanne). 13:828780. doi:10.3389/fendo.2022.828780.

Bownes M. 1992. Why is there sequence similarity between insect yolk proteins and vertebrate lipases? J Lipid Res. 33(6):777–790. doi:10.1016/S0022-2275(20)41504-4.

Bownes M. 1994. The regulation of the yolk protein genes, a family of sex differentiation genes in *Drosophila melanogaster*. Bioessays 16(10):745–752. doi:10.1002/bies.950161009.

Brown EB, Klok J, Keene AC. 2022. Measuring metabolic rate in single flies during sleep and waking states via indirect calorimetry. J Neurosci Methods. 376:109606. doi:10.1016/j.jneumeth.2022.109606.

Burtis KC, Baker BS. 1989. Drosophila Doublesex gene controls somatic sexual differentiation by producing alternatively spliced mRNAs encoding related sex-specific polypeptides. Cell 56(6):997–1010. doi:10.1016/0092-8674(89)90633-8.

Carvalho GB, Kapahi P, Anderson DJ, Benzer S. 2006. Allocrine modulation of feeding behavior by the sex peptide of Drosophila. Curr Biol. 16(7):692–696. doi:10.1016/j.cub.2006.02.064.

Casas-Vila N, Bluhm A, Sayols S, Dinges N, Dejung M, Altenhein T, Kappei D, Altenhein B, Roignant J-Y, Butter F. 2017. The developmental proteome of *Drosophila melanogaster*. Genome Res. 27(7):1273–1285. doi:10.1101/gr.213694.116.

Cermelli S, Guo Y, Gross SP, Welte MA. 2006. The lipid-droplet proteome reveals that droplets are a protein-storage depot. Curr Biol. 16(18):1783–1795. doi:10.1016/j.cub.2006.07.062.

Dauwalder B, Tsujimoto S, Moss J, Mattox W. 2002. The Drosophila takeout gene is regulated by the somatic sex-determination pathway and affects male courtship behavior. Genes Dev. 16(22):2879–2892. doi:10.1101/gad.1010302.

De Groef S, Wilms T, Balmand S, Calevro F, Callaerts P. 2022. Sexual dimorphism in metabolic responses to Western diet in *Drosophila melanogaster*. Biomolecules 12(1):33. doi:10.3390/biom12010033.

Gillette CM, Hazegh KE, Nemkov T, Stefanoni D, D'Alessandro A, Taliaferro JM, Reis T. 2020. Gene–diet interactions: dietary rescue of metabolic defects in spen-depleted *Drosophila melanogaster*. Genetics 214(4):961–975. doi:10.1534/genetics.119.303015.

Gramates LS, Agapite J, Attrill H, Calvi BR, Crosby M, dos Santos G, Goodman JL, Goutte-Gattat D, Jenkins V, Kaufman T. FlyBase: a guided tour of highlighted features. Genetics. 2022;220(4):iyac035.

Gronke S, Mildner A, Fellert S, Tennagels N, Petry S, Müller G, Jäckle H, Kühnlein RP. 2005. Brummer lipase is an evolutionary conserved fat storage regulator in Drosophila. Cell Metab. 1(5):323–330. doi:10.1016/j.cmet.2005.04.003.

Handke B, Poernbacher I, Goetze S, Ahrens CH, Omasits U, Marty F, Simigdala N, Meyer I, Wollscheid B, Brunner E, *et al.* 2013. The hemolymph proteome of fed and starved Drosophila larvae. PLoS One 8(6):e67208. doi:10.1371/journal.pone.0067208.

Haussmann IU, Bodi Z, Sanchez-Moran E, Mongan NP, Archer N, Fray RG, Soller M. 2016. M6a potentiates Sxl alternative pre-mRNA splicing for robust Drosophila sex determination. Nature 540(7632):301–304. doi:10.1038/nature20577.

Hazegh KE, Nemkov T, D'Alessandro A, Diller JD, Monks J, McManaman JL, Jones KL, Hansen KC, Reis T. 2017. An autonomous metabolic role for Spen. PLoS Genet. 13(6):e1006859. doi:10.1371/journal.pgen.1006859.

Hazegh KE, Reis T. 2016. A buoyancy-based method of determining fat levels in Drosophila. J Vis Exp (117):54744. doi:10.3791/54744-v.

Horne I, Haritos VS, Oakeshott JG. 2009. Comparative and functional genomics of lipases in holometabolous insects. Insect Biochem Mol Biol. 39(8):547–567. doi:10.1016/j.ibmb.2009.06.002.

Hoshijima K, Inoue K, Higuchi I, Sakamoto H, Shimura Y. 1991. Control of doublesex alternative splicing by transformer and transformer-2 in Drosophila. Science 252(5007):833–836. doi:10.1126/science.1902987.

Hudry B, de Goeij E, Mineo A, Gaspar P, Hadjieconomou D, Studd C, Mokochinski JB, Kramer HB, Plaçais PY, Preat T, *et al.* 2019 Sex differences in intestinal carbohydrate metabolism promote food intake and sperm maturation. Cell 178(4):901–918 e916. doi:10.1016/j.cell.2019.07.029.

Isaac RE, Li C, Leedale AE, Shirras AD. 2010. Drosophila male sex peptide inhibits siesta sleep and promotes locomotor activity in the post-mated female. Proc Biol Sci. 277(1678):65–70. doi:10.1098/rspb.2009.1236.

Kan L, Grozhik AV, Vedanayagam J, Patil DP, Pang N, Lim K-S, Huang Y-C, Joseph B, Lin C-J, Despic V, *et al.* 2017. The m6A pathway facilitates sex determination in Drosophila. Nat Commun. 8(1):15737. doi:10.1038/ncomms15737.

Kerkis J. 1931. The growth of the gonads in *Drosophila melanogaster*. Genetics 16(3):212–224. doi:10.1093/genetics/16.3.212.

Knuckles P, Lence T, Haussmann IU, Jacob D, Kreim N, Carl SH, Masiello I, Hares T, Villaseñor R, Hess D, *et al.* 2018. Zc3h13/Flacc is required for adenosine methylation by bridging the mRNA-binding factor Rbm15/Spenito to the m(6)A machinery component Wtap/Fl(2)d. Genes Dev. 32(5–6):415–429. doi:10.1101/gad.309146.117.

Koppik M, Fricke C. 2022. Sex peptide receipt alters macronutrient utilization but not optimal yeast-sugar ratio in *Drosophila melanogaster* females. J Insect Physiol. 139:104382. doi:10.1016/j.jinsphys.2022.104382.

Kubrak O, Koyama T, Ahrentløv N, Jensen L, Malita A, Naseem MT, Lassen M, Nagy S, Texada MJ, Halberg KV, *et al.* 2022. The gut hormone Allatostatin C/Somatostatin regulates food intake and metabolic homeostasis under nutrient stress. Nat Commun. 13(1):692. doi:10.1038/s41467-022-28268-x.

Lence T, Akhtar J, Bayer M, Schmid K, Spindler L, Ho CH, Kreim N, Andrade-Navarro MA, Poeck B, Helm M, *et al.* 2016. M6a modulates neuronal functions and sex determination in Drosophila. Nature 540(7632):242–247. doi:10.1038/nature20568.

Link JC, Chen X, Arnold AP, Reue K. 2013. Metabolic impact of sex chromosomes. Adipocyte 2(2):74–79. doi:10.4161/adip.23320.

Liu P, Ewald J, Pang Z, Legrand E, Jeon YS, Sangiovanni J, Hacariz O, Zhou G, Head JA, Basu N, *et al.* 2023. Expressanalyst: a unified platform for RNA-sequencing analysis in non-model species. Nat Commun. 14(1):2995. doi:10.1038/s41467-023-38785-y.

Love MI, Huber W, Anders S. 2014. Moderated estimation of fold change and dispersion for RNA-seq data with DESeq2. Genome Biol. 15(12):550. doi:10.1186/s13059-014-0550-8.

Lyne R, Smith R, Rutherford K, Wakeling M, Varley A, Guillier F, Janssens H, Ji W, Mclaren P, North P, *et al.* 2007. FlyMine: an integrated database for Drosophila and Anopheles genomics. Genome Biol. 8(7):R129. doi:10.1186/gb-2007-8-7-r129.

Mauvais-Jarvis F. 2015. Sex differences in metabolic homeostasis, diabetes, and obesity. Biol Sex Differ. 6(1):14. doi:10.1186/s13293-015-0033-y.

Mosher J, Zhang W, Blumhagen RZ, D'Alessandro A, Nemkov T, Hansen KC, Hesselberth JR, Reis T. 2015. Coordination between Drosophila Arc1 and a specific population of brain neurons regulates organismal fat. Dev Biol. 405(2):280–290. doi:10.1016/j.ydbio.2015.07.021.

Pang Z, Zhou G, Ewald J, Chang L, Hacariz O, Basu N, Xia J. 2022. Using MetaboAnalyst 5.0 for LC–HRMS spectra processing, multi-omics integration and covariate adjustment of global metabolomics data. Nat Protoc. 17(8):1735–1761. doi:10.1038/s41596-022-00710-w.

Parisi M, Li R, Oliver B. 2011. Lipid profiles of female and male Drosophila. BMC Res Notes. 4(1):198. doi:10.1186/1756-0500-4-198.

Patro R, Duggal G, Love MI, Irizarry RA, Kingsford C. 2017. Salmon provides fast and bias-aware quantification of transcript expression. Nat Methods. 14(4):417–419. doi:10.1038/nmeth.4197.

Reddiex AJ, Gosden TP, Bonduriansky R, Chenoweth SF. 2013. Sex-specific fitness consequences of nutrient intake and the evolvability of diet preferences. Am Nat. 182(1):91–102. doi:10.1086/670649.

Reis T, Van Gilst MR, Hariharan IK. 2010. A buoyancy-based screen of Drosophila larvae for fat-storage mutants reveals a role for Sir2 in coupling fat storage to nutrient availability. PLoS Genet. 6(11):e1001206. doi:10.1371/journal.pgen.1001206.

Reisz JA, Zheng C, D'Alessandro A, Nemkov T. 2019. Untargeted and semi-targeted lipid analysis of biological samples using mass spectrometry-based metabolomics. Methods Mol Biol. 1978:121–135. doi:10.1007/978-1-4939-9236-2_8.

Rideout EJ, Narsaiya MS, Grewal SS. 2015. The sex determination gene transformer regulates male-female differences in Drosophila body size. PLoS Genet. 11(12):e1005683. doi:10.1371/journal.pgen.1005683.

Salisbury DA, Casero D, Zhang Z, Wang D, Kim J, Wu X, Vergnes L, Mirza AH, Leon-Mimila P, Williams KJ, *et al.* 2021. Transcriptional regulation of N6-methyladenosine orchestrates sex-dimorphic metabolic traits. Nat Metab. 3(7):940–953. doi:10.1038/s42255-021-00427-2.

Schwasinger-Schmidt TE, Kachman SD, Harshman LG. 2012 Evolution of starvation resistance in *Drosophila melanogaster*: measurement of direct and correlated responses to artificial selection. J Evol Biol. 25(2):378–387. doi:10.1111/j.1420-9101.2011.02428.x.

Senyilmaz D, Virtue S, Xu X, Tan CY, Griffin JL, Miller AK, Vidal-Puig A, Teleman AA. 2015. Regulation of mitochondrial morphology and function by stearoylation of TFR1. Nature 525(7567):124–128. doi:10.1038/nature14601.

Shaw PJ, Cirelli C, Greenspan RJ, Tononi G. 2000. Correlates of sleep and waking in *Drosophila melanogaster*. Science 287(5459):1834–1837. doi:10.1126/science.287.5459.1834.

Shingleton AW, Vea IM. 2023. Sex-specific regulation of development, growth and metabolism. Semin Cell Dev Biol. 138:117–127. doi:10.1016/j.semcdb.2022.04.017.

Sieber MH, Spradling AC. 2015. Steroid signaling establishes a female metabolic state and regulates SREBP to control oocyte lipid accumulation. Curr Biol. 25(8):993–1004. doi:10.1016/j.cub.2015.02.019.

Sieber MH, Thummel CS. 2012. Coordination of triacylglycerol and cholesterol homeostasis by DHR96 and the Drosophila LipA homolog magro. Cell Metab. 15(1):122–127. doi:10.1016/j.cmet.2011.11.011.

Sivachenko A, Gordon HB, Kimball SS, Gavin EJ, Bonkowsky JL, Letsou A. 2016. Neurodegeneration in a Drosophila model of adrenoleukodystrophy: the roles of the Bubblegum and Double bubble acyl-CoA synthetases. Dis Model Mech. 9(4):377–387. doi:10.1242/dmm.022244.

Sonnenblick BP. 1941. Germ cell movements and sex differentiation of the gonads in the Drosophila embryo. Proc Natl Acad Sci U S A. 27(10):484–489. doi:10.1073/pnas.27.10.484.

Szafer-Glusman E, Giansanti MG, Nishihama R, Bolival B, Pringle J, Gatti M, Fuller MT. 2008. A role for very-long-chain fatty acids in furrow ingression during cytokinesis in Drosophila spermatocytes. Curr Biol. 18(18):1426–1431. doi:10.1016/j.cub.2008.08.061.

Thimgan MS, Seugnet L, Turk J, Shaw PJ. 2015. Identification of genes associated with resilience/vulnerability to sleep deprivation and starvation in Drosophila. Sleep 38(5):801–814. doi:10.5665/sleep.4680.

Vargas MA, Luo N, Yamaguchi A, Kapahi P. 2010. A role for S6 kinase and serotonin in postmating dietary switch and balance of nutrients in *D. melanogaster*. Curr Biol. 20(11):1006–1011. doi:10.1016/j.cub.2010.04.009.

Wat LW, Chao C, Bartlett R, Buchanan JL, Millington JW, Chih HJ, Chowdhury ZS, Biswas P, Huang V, Shin LJ, *et al.* 2020. A role for triglyceride lipase brummer in the regulation of sex differences in Drosophila fat storage and breakdown. PLoS Biol. 18(1): e3000595. doi:10.1371/journal.pbio.3000595.

Wat LW, Chowdhury ZS, Millington JW, Biswas P, Rideout EJ. 2021. Sex determination gene transformer regulates the male-female difference in Drosophila fat storage via the adipokinetic hormone pathway. eLife 10:e72350. doi:10.7554/eLife.72350.

White K, Humphrey D, Hirth F. 2010. The dopaminergic system in the aging brain of Drosophila. Front Neurosci. 4:205. doi:10.3389/fnins.2010.00205.

Yan D, Perrimon N. 2015. Spenito is required for sex determination in *Drosophila melanogaster*. Proc Natl Acad Sci U S A. 112(37): 11606–11611. doi:10.1073/pnas.1515891112.

Editor: D. Drummond-Barbosa